MATERIAL ANALYSIS BY INFRARED MICROIMAGING

Richard T. Carl and Matthew J. Smith

Nicolet Instrument Corporation
5225-1 Verona Rd
Madison, WI 53711-0508

INTRODUCTION

During the past few years, infrared microspectroscopy has progressed from an exotic and difficult technique to a routine method of analysis. This is due to the merger of highly sensitive Fourier transform infrared spectrometers with precision infrared and optical microscopes. Infrared microspectroscopy is now a widely used technique in the fields of failure analysis, forensic chemistry and polymer science. Typically, an experiment would involve obtaining a single infrared spectrum of a trace contaminate or investigation of a single polymer defect.

Recently, there has been an interest in using the infrared microscope as an imaging probe [1-4]. Imaging techniques are used in technologies such as electron microprobes [5], laser electron microscopy [6], surface enhanced Raman spectroscopy [7], and nuclear magnetic resonance [8]. The infrared imaging experiment begins by adding a computer-controlled, two-dimensional motorized stage to an infrared microscope. A series of infrared spectra can then be obtained at specific X and Y positions of the sample. This four-dimensional data array (X vs Y vs frequency vs intensity) can be compressed to three dimensions by choosing a specific frequency for examination. Therefore, a single image will represent the change of intensity of a specific frequency over the spatial range of the sample. A series of images based on different functional groups can be obtained by varying the frequency to be displayed. These Functional Group Images (FGI) [1,4] provide a means of non-destructive evaluation of the chemical composition of a sample on microscopic scale. Non-destructive testing is of particular importance in the coating industry since removal of the coating changes the physical and/or chemical composition of the sample. With the use of infrared microimaging, the sample can be investigated without removal from its physical environs.

EXPERIMENTAL

All data were collected on a Nicolet System 740 spectrometer interfaced to an IR-PLAN™ microscope equipped with a proprietary Nicolet high-sensitivity, narrow band 0.25mm MCT detector. A Spectra-Tech 6" x 6" X-Y motorized stage was mounted on the microscope along with a 15X Cassegrainian objective (0.58 Numerical Aperture). All collection, stage movement and data reduction routines were controlled by the Nicolet data station. All spectra were collected at 8 cm^{-1} resolution using 128 co-added scans for a measurement time of 22 seconds. Redundant Aperturing™ was used in every case to collect spectra of high spatial purity and photometric accuracy [9]. Coated steels, paper and silicon wafer samples were obtained from industrial sources.

Review of Progress in Quantitative Nondestructive Evaluation, Vol. 9
Edited by D.O. Thompson and D.E. Chimenti
Plenum Press, New York, 1990

RESULTS

Coated Steel

The first sample investigated was a section of steel coated with an organic material. This proprietary material was applied to the steel as a corrosion inhibitor. Minimizing the thickness of the coating to the point where the material would still retain its anti-corrosive properties would could reduce costs in the production of this material. A tedious, destructive, wet gravimetric method could be used to determine the coating thickness. Unfortunately, this procedure would only yield an average thickness and large variations in the thickness could still lead to ineffectual protection. Therefore, the purpose of performing an infrared imaging experiment on this sample was to determine the variation of the coating thickness in order to tailor the production process for consistency.

As a first step in setting up the infrared imaging experiment, the bulk sample (75 x 100 mm) was mounted on the X-Y stage. Originally intended to study the effects of weathering, only half of the steel surface was coated while the other half remained uncoated. For this study, both the aperture size and stage step size was set to 400 μm. The area that to be investigated was approximately 0.8 mm square. Thus, the spectrometer was set up to collect a 20 x 20 spectral matrix. The infrared microscope was set up to collect data in the reflectance mode since the steel is a highly reflecting substrate. A new background on the uncoated portion of the the steel was collected after each row (X-varied, Y-fixed) of sample spectra had been collected. This was to minimize any effect of purge changes over the several hours of data collection.

After all the spectra were collected and processed, an individual spectrum was examined to determine the absorption frequency for analysis. The peak height of a band in the C-H stretching region was selected as diagnostic of the coating thickness. A contour plot of the result is shown in Figure 1. This plot represents 400 spectra taken over a sample area of 0.8 x 0.8 mm. The bottom portion of the plot shows no infrared activity for the frequency selected since this is the uncoated portion of the steel surface. At approximately 2000 μm in the Y-direction, the contour lines begin and are closely spaced. This indicates an area of rapidly increasing intensity which should correspond to the edge of the coating. The contour lines soon become more widely spaced indicating the coating is being sampled. An axonometric projection of the contour plot is shown in Figure 2. As can be seen, there is variation throughout this coated area. The smallest peak height is 0.04A and the largest is 0.09A. This corresponds to a variation of over 100%. This variation is in excess of manufacturing specifications for this product.

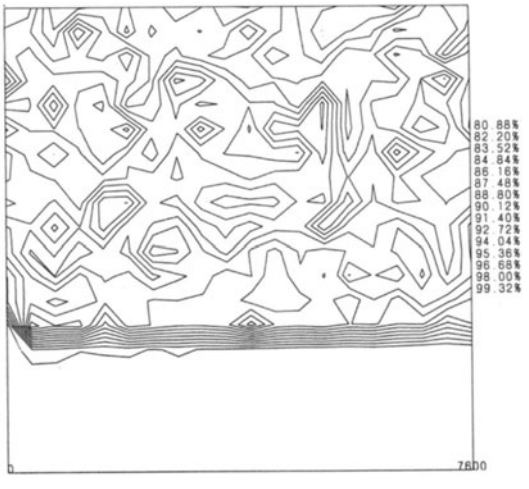

Fig. 1. Contour display of coating on steel surface (Step size: 400 x 400 μm, peak height).

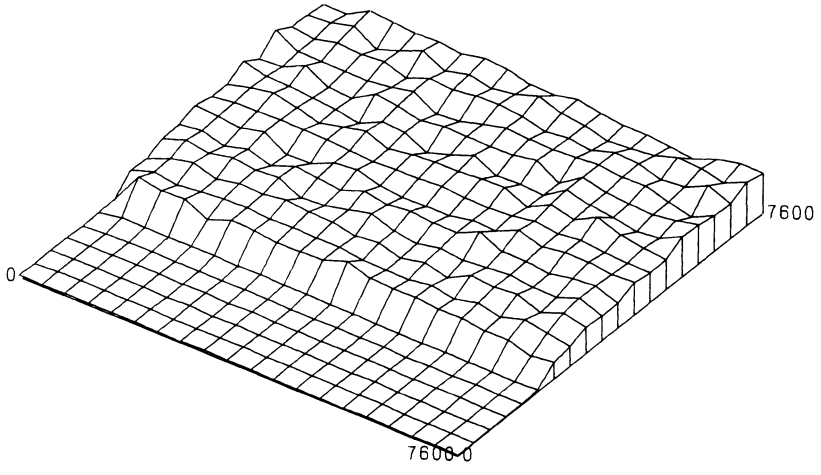

Fig. 2. Axonometric display of coating on steel surface (Step size: 400 x 400 µm, peak height).

In order to investigate the variation on a smaller scale, the aperture and step size were set to 100 µm. A 20 x 20 matrix was collected and the data compression performed using the same C-H stretching frequency. The contour and axonometric projection are shown in Figures 3 and 4. Since the area sampled was only 0.2 x 0.2 mm, the variation in thickness is less than in the previous case. However, the edge of the coating is being explored in much more detail. As can be seen in Figures 3 and 4, there is a gradual slope from the uncoated portion of the steel to the maximum coated level. This can be used as a indication of the speed of the curing process. A rapidly cured product would have a very steep slope since the curing would be completed before the product had a chance to cold flow. A slow cured product would likewise have a gentle slope since a large amount of flow would occur before the product completely cured.

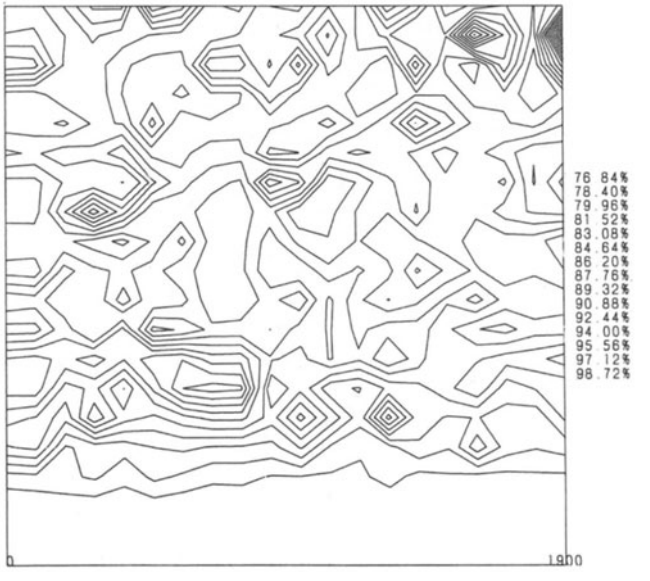

Fig. 3. Contour display of coating on steel surface (Step size: 100 x 100 µm, peak height).

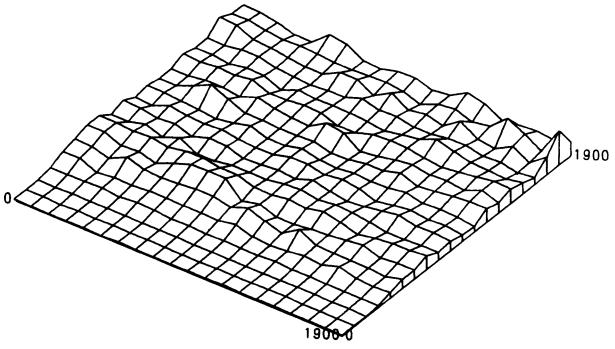

Fig. 4. Axonometric display of coating on steel surface (Step size: 100 x 100 μm, peak height).

Latex Coated Paper

The second product examined was a latex coated paper sample. This product had failed one of the quality control inspection tests after it was manufactured. This particular test consists of applying ink to the coated side of the paper and monitoring for evenness of the ink surface. When the ink appears blotchy or mottled, there is an indication of product failure. The question arose as to whether the mottled appearance comes from the bulk paper or the latex coating. Previously studies using ultra-violet (UV) imaging have indicated that variations in the latex coating will give rise to the mottled appearance [10]. Additional surface studies of latex coated papers have used techniques such as electron spectroscopy for chemical analysis (ESCA) [11] and electron probe x-ray microanalysis [12]. In this case, infrared imaging was used to determine if there are differences in the latex uniformity which could possibly cause mottling during the ink test.

A sample was removed from the paper sheet that had failed the ink test. Initial studies on the microscope on the transmission mode indicated that portions of the infrared spectrum would be totally absorbed due to the thickness of the paper. However, a band at 1509 cm^{-1} could be identified as being due to the latex coating by comparison with a pure spectrum of the latex. The area to be mapped was 4 x 4 mm with a step size of 200 μm. The dual apertures on the microscope were also set to 200 μm. A 20 x 20 spectral matrix was collected over a four hour time period. The data reduction was performed by analyzing the peak area of the 1509 cm^{-1} band. A plot of the contour map is shown in Figure 5 and indicates there is variation in the thickness of the latex coating. The axonometric plot is shown in Figure 6. These results indicate that this latex variation may be causing the mottling in the ink test. Additional work on a sample that passed the quality control test is still needed to confirm this postulate.

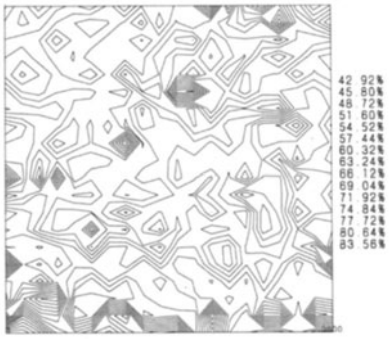

Fig. 5. Contour display of latex coating on paper (Step size: 200 x 200 μm, peak area).

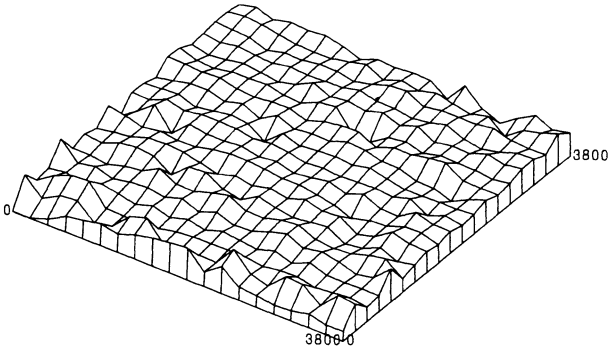

Fig. 6. Axonometric display of latex coating on paper (Step size: 200 x 200 μm, peak area).

Photoresist on Silicon Wafer

In semiconductor processing, polymeric materials known as photoresists are etched to form patterns (pattern etching) which serve as chemical screens to either pass or block high energy ions from reaching the silicon substrate during the ion implantation process. After each successive implantation step, hydrochloric and sulfuric acids are used to etch the material away (final etch) from the surface in preparation for a new application of photoresist. Acid-etch time, for both the final and pattern etch phases, is strickly dependent upon the thickness of the applied photoresist. Therefore, it is highly desirable to maintain the thickness of the material to a predetermined value in order to accurately calculate the required etch time. Therefore, the purpose of performing an infrared imaging experiment on this sample was to determine the variation of the coating thickness in order to tailor the production process.

The area that to be investigated was approximately 0.8 mm by 7.2 mm. Thus, the spectrometer was set up to collect a 20 x 18 spectral matrix. The infrared microscope was set up to collect data in the reflectance mode since the wafer is a highly reflecting substrate. A background on the uncoated wafer was collected prior to the mapping analysis. After all

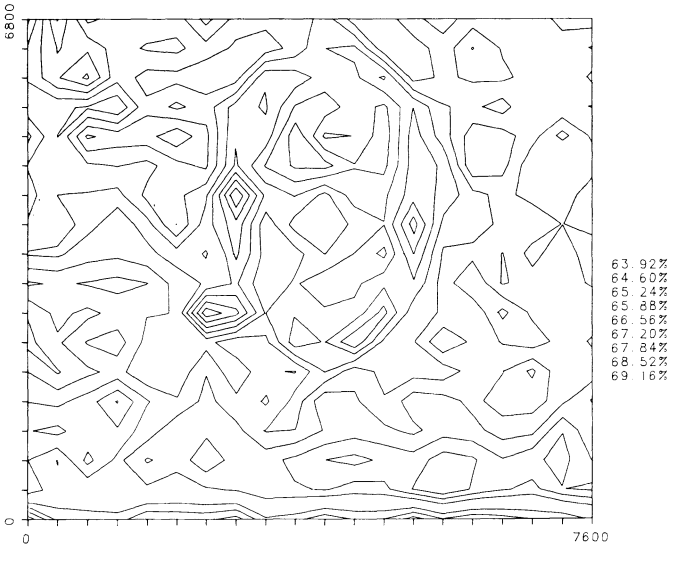

Fig. 7. Contour display of photoresist on silicon wafer (Step size: 400 x 400 μm, peak area).

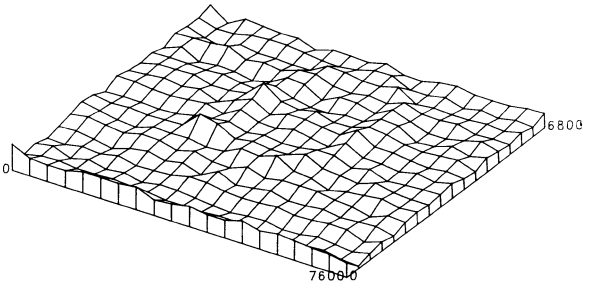

Fig. 8. Axonometric display of photoresist on silicon wafer (Step size: 400 x 400 μm, peak area).

the spectra were collected and processed, an individual spectrum was examined to determine the absorption frequency for analysis. A band in the C-O stretching region was selected as diagnostic of the photoresist thickness. A contour plot of the result is shown in Figure 7. This plot represents 400 spectra taken over a sample area of 0.8 x 0.72 mm. An axonometric projection of the contour plot is shown in Figure 8. As can be seen, there is variation throughout the coated area. The smallest peak height is 0.04A and the largest is 0.09A. This corresponds to a variation of over 100%.

CONCLUSIONS

The coupling of an infrared microscope with a motorized X-Y stage allows the technique of infrared imaging to be performed. Ease of use is facilitated by having flexible software available on the spectrometer data station which can execute rapid data reduction and displays. The application of infrared imaging in both reflectance and transmission can yield valuable information as to the thickness and variation of coatings.

REFERENCES

1. M. A. Harthcock, S. C. Atkin, Appl. Spectros. 42: 449, 1988.
2. M. A. Harthcock, S. C. Atkin, B. L. Davis, "Infrared microspectroscopy functional group imaging as a probe into the compositional heterogeneity of polymer blends," Microbeam Analysis --1988 , 203, 1988.
3. M. A. Harthcock, S. C. Atkin, "Infrared Microspectroscopy: Development and Applications of Imaging Capabilities," in R. G. Messerschmidt and M. A. Harthcock, Eds., Infrared Microspectroscopy: Theory and Applications, New York: Marcel Decker, 21, 1988.
4. M. A. Harthcock and S. C. Atkin, "Compositional mapping with the use of functional group images obtained by infrared microprobe spectroscopy, Microbeam Analysis --1987, 173, 1987.
5. R. B. Marienenko, R. L. Myklebust, D. S. Bright, and D. E. Newbury, Microbeam Analysis --1985, 159, 1985.
6. T. J. Manuccia, Paper #630, Federation of Analytical Chemistry and Spectroscopy Societies Meeting XIII, 1986.
7. R. P. Van Duyne, K. L. Haller, and R. I. Altkorn, Chem. Phys. Lett., 126: 190, 1986.
8. S. L. Smith, in S.A. Borman, Ed., Instrumentation in Analytical Chemistry, Washington, D. C.: American Chemical Society, 303, 1986.
9. R. G. Messerschmidt, "Minimizing Optical Non-Linearities in Infrared Microspectroscopy" in R. G. Messerschmidt and M. A. Harthcock, Eds., Infrared Microspectroscopy: Theory and Applications, New York: Marcel Decker, 1, 1988.
10. H. Fujiwara and J. E. Kline, Tappi J., 97, 1987.
11 H. Tomimasu, S. Ogawa, Y. Sakai, T. Yamasake, and T. Ogura, in Coating Conference Proceedings, Atlanta, Tappi Press, 35, 1986.
12. T. Hamada, M. Khone, Japan Tappi, 39: 43, 1985.